Chemical reactivation of fluorescein isothiocyanate immunofluorescence-labeled resin-embedded samples

Longhui Li
Gong Rao
Xiaohua Lv
Ruixi Chen
Xiaofeng Cheng
Xiaojun Wang
Shaoqun Zeng
Xiuli Liu

SPIE.

Chemical reactivation of fluorescein isothiocyanate immunofluorescence-labeled resin-embedded samples

Longhui Li,[a,b] **Gong Rao,**[a,b] **Xiaohua Lv,**[a,b]
Ruixi Chen,[a,b] **Xiaofeng Cheng,**[a,b] **Xiaojun Wang,**[a,b]
Shaoqun Zeng,[a,b] **and Xiuli Liu**[a,b,*]
[a]Huazhong University of Science and Technology, Wuhan National Laboratory for Optoelectronics, Britton Chance Center for Biomedical Photonics, Wuhan, China
[b]Huazhong University of Science and Technology, MoE Key Laboratory for Biomedical Photonics, Collaborative Innovation Center for Biomedical Engineering, School of Engineering Sciences, Wuhan, Hubei, China

Abstract. Resin embedding is widely used and facilitates microscopic imaging of biological tissues. In contrast, quenching of fluorescence during embedding process hinders the application of resin embedding for imaging of fluorescence-labeled samples. For samples expressing fluorescent proteins, it has been demonstrated that the weakened fluorescence could be recovered by reactivating the fluorophore with alkaline buffer. We extended this idea to immunofluorescence-labeling technology. We showed that the fluorescence of pH-sensitive fluorescein isothiocyanate (FITC) was quenched after resin embedding but reactivated after treating by alkaline buffer. We observed 138.5% fluorescence preservation ratio of reactivated state, sixfold compared with the quenched state in embedding resin, which indicated its application for fluorescence imaging of high signal-to-background ratio. Furthermore, we analyzed the chemical reactivation mechanism of FITC fluorophore. This work would show a way for high-resolution imaging of immunofluorescence-labeled samples embedded in resin. © *The Authors. Published by SPIE under a Creative Commons Attribution 3.0 Unported License. Distribution or reproduction of this work in whole or in part requires full attribution of the original publication, including its DOI.* [DOI: 10.1117/1.JBO.23.2.020501]

Resin-embedding technology is widely used and facilitates microscopic imaging of biological tissues.[1] Fluorescence-labeling technology helps visualizing the localization of specific proteins and fine structures in cells and tissues.[2,3] Conventionally, the fluorophores of tissue samples would be quenched or attenuated during resin-embedding process,[4–6] this makes it difficult to combine resin-embedding methods with fluorescence labeling techniques. For samples expressing fluorescent proteins, like enhanced green/yellow fluorescent protein (EGFP/EYFP) and pHuji, it was demonstrated that fluorescence decayed after resin embedding because of fluorophore protonation during embedding process, and treating with alkaline buffer could change most of the fluorophores to fluorescent anionic state by deprotonating and then enhanced fluorescence intensity of specimen during imaging.[7,8] This method was named chemical reactivation (CR), which has realized combining the advantages of fluorescent protein-labeling and resin-embedding technologies in fluorescence microscopic imaging of biological tissues.[7–9]

Immunofluorescence labeling is another important technology aimed at acquiring the profile of biomolecules, especially those difficult to be labeled by fluorescent proteins. In previous study, researchers sliced the resin-embedded tissues first, collected, stained, and imaged the slices later.[10] Recently, iDISCO immunostaining technique has brought revolutionary breakthrough in en bloc immunofluorescence labeling,[11] and based on it, researchers combined immunofluorescence labeling with resin embedding to visualize three-dimensional (3-D) biomolecule distribution information of immunolabeled large tissues with high resolution.[12] To succeed, they have evaluated the fluorescence behavior of commonly used fluorescent probes in commonly used resins and then screened out the suitable combinations for fluorescence imaging.

Here, we propose an idea using pH-sensitive fluorescent probe for immunofluorescence labeling and CR to recover fluorescence intensity after resin embedding. Since fluorescein isothiocyanate (FITC) had a high fluorescence quantum yield[13,14] and was widely used for monitoring pH values [15–17] and immunofluorescence labeling of biological tissues,[18–22] we chose FITC as one representative of pH-sensitive fluorescent probe to realize the idea. First, we investigated whether the fluorescence of FITC would be quenched during resin-embedding process, then further tested whether the quenched immunofluorescence could be reactivated. Subsequently, we studied the fluorescence spectra of FITC fluorophores (containing the absorption, excitation, and emission spectra) under different pH conditions in resin polymers compared with those in aqueous solutions. Finally, we analyzed the molecular structure and CR mechanism of FITC fluorophore embedded in resin.

The biological tissues immunostaining and resin-embedding procedures followed previous research.[11] Eight-week-old C57BL/6J mice were used in this research. Animal care and use were in accordance with the guidelines of the Administration Committee of Affairs Concerning Experimental Animals in Hubei Province of China. The protocol was approved by the Committee on the Ethics of Animal Experiments of the Huazhong University of Science and Technology (Permit Number: 00027340). All efforts were made to minimize the suffering of the animals. The mice were anesthetized and intracardially perfused with 0.01-M phosphate buffered saline (PBS, Sigma–Aldrich), and then postfixed in 4% paraformaldehyde (Sigma–Aldrich) for 24 h. The brains were sliced to 70-μm sections using a vibration microtome (VT1000 S, Leica) for FITC immunofluorescence labeling. After being rinsed in 0.01-M PBS (Sigma) for 5 min two times, the slices were blocked in PBS/0.2% Triton X-100/10% goat serum (Boster Biological Technology) at room temperature for 2 h. Subsequently, slices

were incubated with primary antibody (mouse anti GFAP, Abcam) dilutions in PBS/0.2% Triton X-100/10% goat serum at 4°C with gentle shaking on an oscillator for overnight, and rinsed for 5 min with 0.01-M PBS five times. Finally, the slices were incubated with secondary antibody (FITC goat antimouse polyclonal antibody, Jackson) dilutions in PBS/0.2% Triton X-100 at 37°C with gentle shaking on an oscillator for 2 h, and rinsed in 0.01-M PBS 5 min five times. After immunostaining, the slices were transferred to imaging and then resin embedding. For imaging, we utilized confocal microscope (LSM780, Zeiss, using 488 nm laser and 20× water immersion objective, N.A. 1.0) to image the FITC immunofluorescence-labeled astrocytes of brain slices in 0.01-M PBS. For resin embedding with GMA (Technovit 8100, Electron Microscopy Sciences), the brain slices were treated with a graded ethanol series (30%, 50%, 75%, 85%, 95%, 100%, 100%, and 100%, 10 min each time at 4°C), followed by GMA resin monomer three times (10 min at 4°C), then placed on glass slides with GMA polymerization solution, sealed with coverslips, and finally the brain slices polymerized at 4°C for 12 h.

We evaluated quantitatively the fluorescence preservation ratios of FITC immunofluorescence-labeled astrocytes of brain slices when embedded and when chemically reactivated by alkaline solutions, utilizing the same aforementioned confocal microscope and system parameters. The fluorescence image of the FITC immunofluorescence-labeled astrocytes in 0.01 M PBS was shown in Fig. 1(a), from the figure we can see the fluorescence was bright enough to visualize fine structures of astrocytes. We found that the same astrocytes after GMA embedding were quenched badly with weak fluorescence observed under the same imaging condition [Fig. 1(b)], and
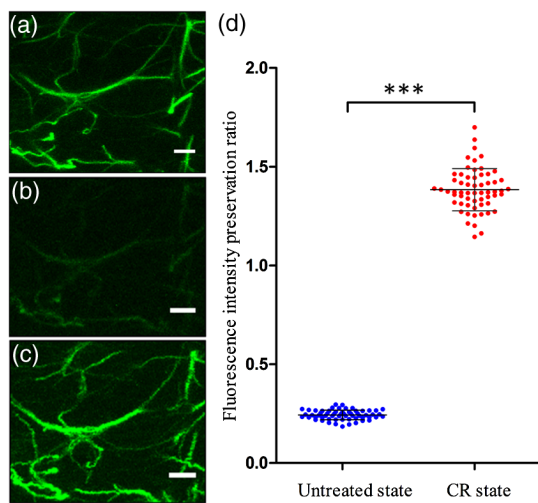
named this state untreated state, which was before CR using alkaline buffer. Subsequently, we treated the quenched slices with alkaline buffer (Na$_2$CO$_3$ solution, pH = 10, 100 μL) for CR. The alkaline buffer penetrated into the slices through the micropores of GMA polymer and reactivated the FITC fluorophores inside. After 5 min, the quenched FITC was reactivated and the fluorescent intensity was detected [Fig. 1(c)], and this state was named CR state. Then, we calculated the mean value of all the pixels in the images to represent the fluorescence intensity of the same astrocyte in different states and quantitatively analyzed the fluorescence preservation ratios of astrocytes in untreated state and CR state compared with them in 0.01-M PBS solution state. We obtained 24.3% $\pm$ 2.4% ($n = 60$ astrocytes from four brain slices, mean $\pm$ SD) fluorescence preservation ratio of untreated state and 138.5% $\pm$ 10.7% ($n = 60$ astrocytes from four brain slices, mean $\pm$ SD) fluorescence preservation ratio of CR state [Fig. 1(d)]. Data were statistically analyzed with paired-samples two-tailed t-test, and the result showed there was a significant difference ($p < 0.0001$), which demonstrated that the fluorescence intensity of FITC immunofluorescence-labeled specimens was quenched during resin-embedding process but significantly improved after CR.

We studied the fluorescence spectra of FITC fluorophores under different pH conditions in resin polymers compared with those in aqueous solutions. Here, in our study of FITC fluorophore in resin polymer, the pure FITC (Sigma) was dissolved in GMA resin monomer (10^{-5} mol/L) and polymerized on a group of glass slides at 4°C for 12 h. The control group was a group of FITC aqueous solutions (10^{-6} mol/L) in different pH conditions. The absorption spectra (LabRAM HR800 UV/vis spectrophotometer, Horiba JobinYvon), fluorescence excitation (emission wavelength 525 nm) and emission spectra (excitation wavelength 488 nm, FP-6500 Spectrofluorometer, Jasco) were shown in Fig. 2. Unapparent absorption, fluorescence excitation, and emission spectra in untreated state were detected [Figs. 2(a) and 2(c)]. When treated by a series of pH buffers, the FITC fluorophores in GMA polymers had significant absorption, fluorescence excitation and emission at weakly acidic, neutral, and alkaline pH (pH 5 to 11) [Figs. 2(a) and 2(c)], more or less identical to FITC aqueous solutions (pH 5 to 11) [Figs. 2(b) and 2(d)], whereas much smaller absorption, fluorescence excitation and emission of FITC at acidic condition (pH 3 to 4) in GMA polymers compared with FITC aqueous solutions (pH 3 to 4, absorption and excitation peaks at ~437 nm). Fluorescence excitation and emission spectra of FITC in GMA polymers treated by pH buffers were similar to those of FITC aqueous solutions in shape with excitation peaks at ~499 nm (~494 nm in aqueous solutions) and emission peaks at ~525 nm (~521 nm in aqueous solutions), showing a little redshift. The maximums of spectra happened at condition of pH = 10 (pH = 9 in aqueous solutions), which was most suitable for CR.

The chemical structures and CR mechanism of FITC fluorophore have been analyzed based on previous research.[13,14] In brief, the FITC fluorophore has four dominated protolytic forms, cation (FH$_3^+$), neutral species (FH$_2$), anion (FH$^-$), dianion (F^{2-}),[13,14] which make the fluorescence properties remarkably dependent on pH values [Fig. 3(a)]. [FH$_3^+$]*, [FH$_2$]*, [FH$^-$]*, and [F^{2-}]* represent their excited state after absorbing photons, respectively [Fig. 3(b)]. The protolytic constants in the ground state are pK$_1$ (2.08), pK$_2$ (4.31), and pK$_3$ (6.43),[13] as shown in Fig. 3(b). Only anion and dianion are fluorescent

Fig. 1 CR of FITC immunofluorescence-labeled astrocytes in GMA-embedded mouse brain slices. (a) Fluorescence microimaging of astrocytes in 0.01-M PBS solution state, (b) untreated state (GMA polymer), and (c) CR state (pH = 10 alkaline buffer-treated GMA polymer), respectively. (d) Fluorescence intensity preservation ratios of astrocytes in untreated state and CR state compared with them in 0.01-M PBS solution state are about 24.3% $\pm$ 2.4% ($n = 60$ astrocytes from four brain slices, mean $\pm$ SD) and 138.5% $\pm$ 10.7% ($n = 60$ astrocytes from four brain slices, mean $\pm$ SD), respectively. The results showed that the fluorescence intensity of FITC immunofluorescence-labeled astrocytes was quenched in untreated state but significantly improved after CR ($p < 0.0001$, paired-samples two-tailed t test). Scale bar: 10 μm.
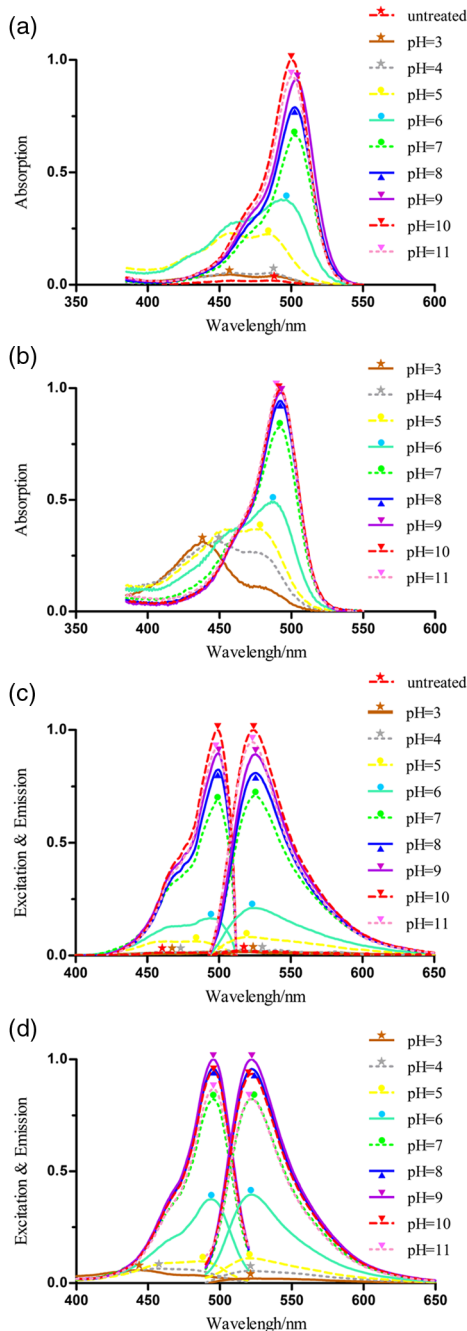
Fig. 2 Fluorescence spectra of FITC. (a) and (b) Absorption spectra of FITC under different pH conditions in GMA polymers and aqueous solutions, respectively. Unapparent absorption spectra of FITC was detected in untreated state and no significant absorption spectra of FITC at acidic condition (pH 3 to 4) in GMA polymers compared with FITC aqueous solutions (pH 3 to 4, peak at ~437 nm). (c) and (d) Fluorescence excitation (emission wavelength 525 nm) and emission spectra (excitation wavelength 488 nm) of FITC under different pH conditions in GMA polymers and aqueous solutions, respectively. Unapparent fluorescence excitation and emission spectra of FITC were detected in untreated state. Much smaller excitation and emission spectra of FITC at acidic condition (pH 3 to 4) in GMA polymers compared with FITC aqueous solutions (pH 3 to 4, excitation peak at ~437 nm). Fluorescence excitation and emission spectra of FITC in GMA polymers treated by pH buffers were similar to those of FITC aqueous solutions in shape with excitation peaks at ~499 nm (~494 nm in aqueous solutions) and emission peaks at ~525 nm (~521 nm in aqueous solutions), showing a little redshift. The maximums of spectra happened at condition of pH = 10 (pH = 9 in aqueous solutions).
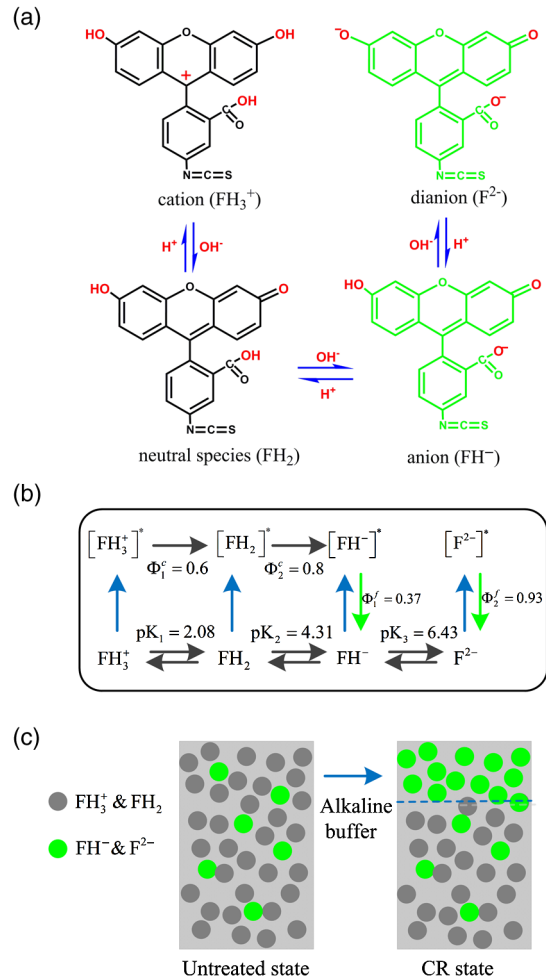

Fig. 3 Chemical structures and CR mechanism of FITC. (a) Four dominated protolytic forms of FITC, cation (FH_3^+), neutral species (FH^2), anion (FH^-), dianion (F^{2-}).[13,14] (b) Ground and excited state reactions of FITC.[13] (c) Schematic of high signal-to-background ratio during fluorescence microimaging using CR. Nonfluorescent cation and neutral species of FITC dominate in resin-embedded sample before CR (left). When the block-surface layer of the sample is treated by alkaline buffer, fluorescent anion, and dianion dominate, significantly increasing fluorescence intensity compared with unprocessed nether layers (right).

species with fluorescence quantum yield of Φ_1^f (0.37) and Φ_2^f (0.93), but the nonfluorescent cation and neutral species in the excited state ($[FH_3^+]^*$, $[FH_2]^*$) could convert into anion ($[FH^-]^*$) in aqueous solutions with conversion yield Φ_1^c (0.6) and Φ_2^c (0.8) [Fig. 3(b)],[13] resulting in a small amount of absorption, fluorescence excitation, and emission [Figs. 2(b) and 2(d)]. However, this conversion hardly happens in resin-embedded FITC fluorophore, according to spectra shown in Figs. 2(a) and 2(c). Furthermore, unapparent absorption, fluorescence excitation, and emission spectra of FITC fluorophores in untreated state [Figs. 2(a) and 2(c)] prove the nonfluorescent cation and neutral species dominate in resin [Fig. 3(c), left], and FITC fluorophore has experienced a transition into nonfluorescent state because of fluorophore protonation during resin-embedding process. However, the resin-embedding process just quenched FITC instead of damaging it, because the quenched FITC could be chemically reactivated by alkaline buffer later [Figs. 2(a) and 2(c)]. It is worth noting that the

fluorescence intensity on the alkaline buffer-treated block-surface layer of tissues was much stronger than unprocessed nether layers [Fig. 3(c), right], thus CR benefits high signal-to-background ratio in fluorescence microscopic imaging by avoiding the out-of-focus interference.

We chose the pH-sensitive FITC fluorescent probe based on the following considerations. First, the FITC fluorescent probe is suitable for CR using alkaline solution. The fluorescent probes exhibiting strong fluorescence in acidic condition but emitting weak fluorescence in alkaline condition are not appropriate for CR of immunofluorescence labeling, because they are reactivated by acidic solution, which may severely affect the antigen–antibody reaction.[23] Second, FITC has a high fluorescence quantum yield, so the fluorescence intensity in CR state is high enough for fluorescence imaging. In the end, FITC is commercially available and widely used in biological study. Immunofluorescence probe, which meets the aforementioned requirements, may be a good candidate for CR in resin-embedded samples.

In conclusion, we demonstrated that the pH-sensitive FITC immunofluorescence-labeled resin-embedded samples could apply CR to efficaciously solve the fluorescence-quenching problem. We found pH = 10 buffer was most suitable for CR of FITC fluorophore. During fluorescence imaging, the $138.5\% \pm 10.7\%$ fluorescence preservation ratio of CR state benefits fine structure imaging of samples, the $24.3\% \pm 2.4\%$ fluorescence preservation ratio of untreated state benefits decreasing background fluorescence interference, thus this work would assure fluorescence imaging of high signal-to-background ratio and shows a potential of 3-D high-resolution imaging of immunofluorescence-labeled samples embedded in resin with the continuously imaging strategy of imaging first and slicing later.

Disclosures

The authors have no relevant financial interests in this article and no potential conflicts of interest to disclose.

Acknowledgments

References

1. S. B. Newman, E. Borysko, and M. Swerdlow, "New sectioning techniques for light and electron microscopy," *Science* **110**(2846), 66–68 (1949).
2. A. H. Coons and M. H. Kaplan, "Localization of antigen in tissue cells; improvements in a method for the detection of antigen by means of fluorescent antibody," *J. Exp. Med.* **91**(1), 1–13 (1950).
3. M. Chalfie et al., "Green fluorescent protein as a marker for gene expression," *Science* **263**(5148), 802–805 (1994).
4. W. W. Ward, "Biochemical and physical properties of green fluorescent protein," *Methods of Biochemical Analysis*, 2nd ed., Vol. **47**, pp. 39–65 (2006).
5. T. Ragan et al., "Serial two-photon tomography for automated ex vivo mouse brain imaging," *Nat. Methods* **9**(3), 255–258 (2012).
6. M. N. Economo et al., "A platform for brain-wide imaging and reconstruction of individual neurons," *Elife* **5**, e10566 (2016).
7. H. Xiong et al., "Chemical reactivation of quenched fluorescent protein molecules enables resin-embedded fluorescence microimaging," *Nat. Commun.* **5**, 3992 (2014).
8. W. Guo et al., "Chemical reactivation of resin-embedded pHuji adds red for simultaneous two-color imaging with EGFP," *Biomed. Opt. Express* **8**(7), 3281–3288 (2017).
9. H. Gong et al., "Continuously tracing brain-wide long-distance axonal projections in mice at a one-micron voxel resolution," *NeuroImage* **74**(7), 87–98 (2013).
10. K. D. Micheva and S. J. Smith, "Array tomography: a new tool for imaging the molecular architecture and ultrastructure of neural circuits," *Neuron* **55**(1), 25–36 (2007).
11. N. Renier et al., "iDISCO: a simple, rapid method to immunolabel large tissue samples for volume imaging," *Cell* **159**(4), 896–910 (2014).
12. Y. Gang et al., "Plastic embedding immunolabeled large-volume samples for three-dimensional high-resolution imaging," *Biomed. Opt. Express* **8**(8), 3583–3596 (2017).
13. R. Sjöback, J. Nygren, and M. Kubista, "Absorption and fluorescence properties of fluorescein," *Spectrochim. Acta, Part A* **51**(6), L7–L21 (1995).
14. T. Maeda et al., "Identification of chemical species of fluorescein isothiocyanate isomer-I (FITC) monolayers on platinum by doubly resonant sum-frequency generation spectroscopy," *J. Raman Spectrosc.* **39**(11), 1694–1702 (2008).
15. S. C. Ritter, M. A. Milanick, and K. E. Meissner, "Encapsulation of FITC to monitor extracellular pH: a step towards the development of red blood cells as circulating blood analyte biosensors," *Biomed. Opt. Express* **2**(7), 2012–2021 (2011).
16. B. Hoffmann and H. Kosegarten, "FITC-dextran for measuring apoplast pH and apoplastic pH gradients between various cell types in sunflower leaves," *Physiol. Plant.* **95**(3), 327–335 (1995).
17. H. Liu et al., "The influence of virus infection on the extracellular pH of the host cell detected on cell membrane," *Front. Microbiol.* **7**, 1127 (2016).
18. N. Dioguardi and E. C. Vigliani, "A fluorescein isothiocyanate (FITC) standard for quantification in immunofluorescence microscopy. Application to microfluorometry of human peripheral blood lymphocyte membrane IgM receptors," *Ric. Clin. Lab.* **5**(2), 128–134 (1975).
19. A. Juarranz et al., "Fluorescent porphyrin counterstaining of chromatin DNA in conjunction with immunofluorescence methods using FITC-labelled antibodies," *J. Microsc.* **182**(1), 46–49 (1996).
20. T. Cowen, "Image analysis of FITC-immunofluorescence histochemistry in perivascular substance P-positive nerves," *Histochemistry* **81**(6), 609–610 (1984).
21. H. G. de Bruin, L. I. De, and C. Aaij, "Quantitative determination of the number of FITC-molecules bound per cell in immunofluorescence flow cytometry," *Vox Sang.* **45**(5), 373–377 (1983).
22. A. Entwistle and M. Noble, "The use of Lucifer yellow, bodipy, FITC, TRITC, RITC and Texas red for dual immunofluorescence visualized with a confocal scanning laser microscope," *J. Microsc.* **168**(3), 219–238 (1992).
23. J. A. Ramosvara, "Technical aspects of immunohistochemistry," *Vet. Pathol.* **42**(4), 405–426 (2005).